JPPIPA 12(1) (2026)

Jurnal Penelitian Pendidikan IPA

http://jppipa.unram.ac.id/index.php/jppipa/index

Landslide Susceptibility Zonation Based on Seismic Vulnerability Index and Subsurface Lithology Derived from Resistivity Values

Ira Jam'iyatul Qalbiyah[1], Adi Susilo[1*], Eko Andi Suryo[2]

[1] Department of Physics, Faculty of Mathematics and Natural Sciences, Brawijaya University, Malang, Indonesia.
[2] Department of Civil Engineering, Faculty of Engineering, Brawijaya University, Malang, Indonesia.

Received: November 27, 2025
Revised: December 23, 2025
Accepted: January 25, 2026
Published: January 31, 2026

Corresponding Author:
Adi Susilo
adisusilo@ub.ac.id

DOI: 10.29303/jppipa.v12i1.13625

Abstract: This study aims to determine potential landslide-prone zones based on the seismic vulnerability index and subsurface lithology derived from electrical rock resistivity values. The research employs the microseismic method and the geoelectric resistivity method with a dipole–dipole configuration. Zones with high landslide susceptibility are identified at points exhibiting high values of the seismic vulnerability index. Based on data acquisition, the highest amplification factor was recorded at point D3 of 9.24, with a corresponding seismic vulnerability index of 24.57. Subsurface lithology analysis reveals an alluvium layer with a thickness of up to 25.00 meters overlying the bedrock. These datasets indicate that the alluvial soil is characterized by soft textures, incomplete consolidation, and low stability levels, rendering these specific points highly vulnerable to significant damage and landslide activity.

Keywords: Alluvial; Dipole-dipole; Geoelectric; Landslide susceptibility; Seismic vulnerability index

Introduction

Landslides represent a major natural disaster that results in significant losses (Y. Chen et al., 2025). They pose a severe threat by endangering infrastructure, communities, and human lives (Stark et al., 2025). Landslides represent a widespread geological phenomenon globally, primarily triggered by the increase of pore water pressure resulting from high precipitation. As climate change intensifies rainfall events, the risk and frequency of landslide occurrences are projected to increase significantly (Moradi et al., 2021). A landslide is defined as the sudden downslope displacement of rock or soil masses under the influence of gravity, triggered by various factors such as intense rainfall, earthquakes, or rapid river erosion (Pourghasemi et al., 2020). Given Indonesia's geological, geographical, hydrometeorological, and demographic conditions, landslides occur frequently, particularly in the Bumiaji District of Batu City.

Landslides are driven by two primary factors: controlling factors and triggering factors. Controlling factors encompass topography, geological structure, environmental conditions, and soil properties (Liao et al., 2022). Meanwhile, triggering factors are categorized into natural and anthropogenic influences (Liao et al., 2022). Among these, rainfall-induced landslides represent a particularly hazardous phenomenon, typically occurring within unsaturated zones (Guo et al., 2021).

Topographically, Bumiaji District is located in a hilly region characterized by numerous steep slopes, making it highly susceptible to landslides during the rainy season (BPS Batu City 2025). According to the BNPB geoportal, recent landslide events have caused significant damage to residential properties due to soil instability and saturation. Based on the regional

How to Cite:
Qalbiyah, I. J., Susilo, A., & Suryo, E. A. Landslide Susceptibility Zonation Based on Seismic Vulnerability Index and Subsurface Lithology Derived from Resistivity Values. *Jurnal Penelitian Pendidikan IPA*, *12*(1), 19-27. https://doi.org/10.29303/jppipa.v12i1.13625

geological map, the study area is situated within the Old Anjasmara Volcanic Rock Formation (Qpat), which consists of volcanic breccia, lava, tuff, and dikes (Masitoh et al., 2019; Santosa et al., 1992). The slope inclination in this area ranges from 13% to 55%, where a steeper slope angle significantly increases the potential for landslide occurrences (Rif'ah et al., 2024). Furthermore, high-altitude regions characterized by weathered soil types and anthropogenic fill structures are highly susceptible to landslides following high-intensity rainfall events (Gbadebo et al., 2021).

The objective of this research is to integrate the seismic vulnerability index and subsurface lithology profiling using a dipole-dipole geoelectric configuration to map landslide risks. This study correlates the dynamic response of microseismic data with subsurface rock resistivity. This dual-method approach enables the identification of potential slip planes and soil fragility levels that cannot be detected through surface observation alone. This research is of critical importance as Bumiaji District is a rapidly developing residential zone despite its steep topography. The findings provide a scientific foundation for early warning systems and safe infrastructure development, ensuring that local residents are better protected from landslide risks by determining the seismic vulnerability index and alluvial thickness.

Method

Type of Research

This study employs an integrated quantitative approach by combining two methods: microseismic and geoelectrical resistivity. This applied approach focuses on disaster mitigation through seismic microzonation mapping and the identification of subsurface lithology. The integration of these two methods aims to delineate landslide vulnerability zones in Gunungsari Village, Bumiaji District.

Research Methods

The methods applied in this research include the HVSR microseismic method and the geoelectrical resistivity method. The integration of these two methods has proven to be the most effective approach for characterizing subsurface structures and the internal mechanisms of landslides, as both techniques are capable of identifying subsurface conditions with high spatial and volumetric precision (Himi et al., 2022). Microseismic activity refers to very low-magnitude seismic wave vibrations, similar to earthquakes but with an intensity too weak to be felt by humans (Haerudin et al., 2019). The microseismic method is utilized to analyze the dynamic characteristics of sediment layers by identifying the dominant frequency and the amplification factor. These two parameters are subsequently used to calculate the seismic vulnerability index. The dominant frequency represents the frequency value of the rock layers in the area, providing information regarding rock types and characteristics (Syamsuddin et al., 2021). Furthermore, the dominant frequency can be influenced by the topographic conditions of the study area (Januarta et al., 2020).

The amplification factor refers to the magnification of seismic waves that occurs as they propagate from a harder medium to a softer one (Yuliawati et al., 2019). This amplification value varies significantly depending on the level of deformation and weathering of the rock body, even within the same rock type (Rananda et al., 2020). Once the dominant frequency and amplification factor are obtained, a new parameter is derived, namely the seismic vulnerability index. The seismic vulnerability index is a parameter that characterizes the degree of susceptibility of the surface soil layer in an area to deformation during an earthquake. Mathematically, Nakamura (2000) formulated the seismic vulnerability index as follows (Alonso-Pandavenes et al., 2023):

$$Kg = \frac{{A_0}^2}{f_0} \quad (1)$$

Where Kg is the seismic vulnerability index, A_0 is the amplification factor, and f_0 is the dominant frequency. The seismic vulnerability index represents the susceptibility of a material to deformation and serves as a parameter to define ground weakness; furthermore, it correlates with the potential instability of landslide-prone areas (Alonso-Pandavenes et al., 2023). Subsequently, these processing results are analyzed to delineate zones that are susceptible to damage. Low damage potential is associated with areas exhibiting a low seismic vulnerability index. Conversely, if the seismic vulnerability index is high, the area is expected to sustain significant damage (Syamsuddin et al., 2021).

The geoelectrical resistivity method is a technique used to characterize the arrangement and depth of rock layers by measuring electrical properties at the ground surface (Novianti, 2019). This method measures subsurface resistivity variations by injecting high-voltage DC current to identify the structure of geological layers (Karimah et al., 2022). In principle, this method is conducted by injecting an electrical current into the ground through current electrodes A and B, and subsequently measuring the potential difference via potential electrodes M and N. From these two parameters, the resistance distribution within a specific medium is obtained using the following equation (Rizzo et al., 2022):

$$\Delta V_{MN} = I_{AB}R \quad (2)$$

Where ΔV is the potential difference between electrodes M and N, I is the current injected into electrodes A and B, and R is the resistance of the material through which the current passes (Rizzo et al., 2022).

According to Arif (2016), a geoelectric resistivity survey involves injecting an electric current into the earth via two current electrodes and measuring the potential difference across two potential electrodes. The resulting measurements yield the resistivity value (or specific resistance) of each layer beneath the surface. In this method, the earth is assumed to be a homogeneous isotropic medium. The injected current flows in all directions, forming hemispherical equipotential surfaces (Hakim et al., 2016). Based on this assumption, the resistivity value measured during data acquisition is the apparent resistivity, which is mathematically expressed as follows (Febriani et al., 2020):

$$\rho_a = k\frac{V}{I} \quad (3)$$

Where, ρ_a is the apparent resistivity value, k is the geometric factor, which varies depending on the specific electrode configuration, V is the potential difference, and I is the electric current.

This configuration provides a subsurface image that is relatively deeper compared to the sounding method utilizing the Wenner-Schlumberger configuration. In the dipole-dipole configuration, electrodes A and B serve as the current electrodes, while electrodes M and N function as the potential electrodes (Yue et al., 2024). In this configuration, the spacing between electrodes is not necessarily equal. The position of the current electrodes is kept fixed, while the potential electrodes move away from the current electrodes up to an optimal distance, typically seven times the electrode spacing (a or n = 7). The separation between the current electrodes and between the potential electrodes is defined by the spacing (a). The pair of potential electrodes is progressively moved until the end of the survey line is reached (Sholichin 2018).

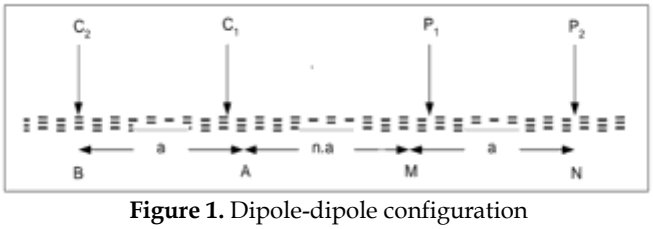

Figure 1. Dipole-dipole configuration

The equation for the geometric factor (k) of the dipole-dipole configuration, where the separation factor n equals 1, 2, 3, … n, is given by Sholichin (2018).

$$k = \pi an(n+1)(n+2) \quad (4)$$

Where, k is the geometric factor, a is the electrode spacing, and n is the separation factor or integer multiple of the spacing to obtain the apparent resistivity (ρ_a) value for the dipole-dipole configuration, the geometric factor (k) from Equation 3 is substituted into Equation 3, resulting in:

$$\rho_\alpha = \pi an(n+1)(n+2)\frac{\Delta V}{I} \quad (5)$$

The dipole-dipole array was employed for its ability to achieve significant penetration depths while maintaining robust resolution of vertical and horizontal geological features. Therefore, this approach proves highly efficient in delineating discontinuities between lithological units and sediments within unstable environments (Zevallos et al., 2025).

Data Collection and Analysis

In this research, the seismic vulnerability index value was obtained from microseismic measurements analyzed using the HVSR method. Conversely, the rock resistivity value was derived from data acquisition using the geoelectric resistivity method. Microseismic data acquisition was conducted in Gunungsari Village, Bumiaji District (Figure 2).

Figure 2. Map of microseismic data acquisition desain

Data acquisition was conducted in Gunungsari Village, Bumiaji District. The instruments utilized for microseismic measurements included a SARA seismometer and a GPS to determine the measurement coordinates. Microseismic data were collected at 20 points, with a duration of 30–45 minutes per point. The acquisition aimed to analyze the seismic vulnerability index at the study site. The data collection procedures strictly adhered to the criteria recommended by SESAME (S. Chen et al., 2023). The recorded signals were processed using Geopsy software to derive the natural frequency and maximum amplitude through HVSR analysis (Krylov et al., 2022). HVSR analysis is employed to determine the dynamic characteristics of sediment

layers, such as the natural frequency and the H/V peak ratio. This analysis is commonly used for seismic microzonation mapping, amplification factors, and seismic vulnerability indices (Susilo et al., 2012). The HVSR method utilizes the FFT algorithm to analyze the spectral ratio of horizontal components relative to the vertical component (Susilo et al., 2026).

The effectiveness of the HVSR method is well-regarded for analyzing soil layer characteristics, supported by its ability to detect natural resonance frequencies, identify soil stratigraphy, and remain cost-effective as it eliminates the need for drilling (Cintia et al., 2024). The data processing yields the HVSR curve, dominant frequency, and amplification factor (Demulawa et al., 2021). These two parameters are subsequently utilized to calculate the seismic vulnerability index for each measurement point. This value serves to identify weak zones on the ground surface. A higher seismic vulnerability index at a measurement point indicates a greater susceptibility of the soil at that location to damage or deformation when subjected to vibrations (Marfai et al., 2018).

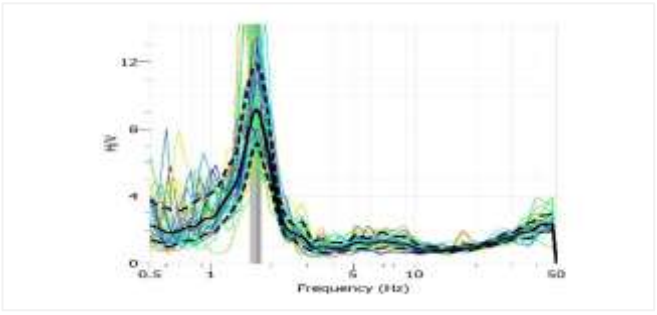

Figure 3. HVSR Curve

After identifying the points with high seismic vulnerability index values, geoelectrical resistivity data acquisition was conducted around those specific areas. The objective of this acquisition was to identify the subsurface lithology surrounding these points. The geoelectrical resistivity data were collected using a MAE resistivity meter across two survey lines, each spanning 160 meters. The acquired data included datum point positions, apparent resistivity values, as well as the coordinates and elevations of each electrode position. The field data were subsequently processed using Res2Dinv software (Zhang et al., 2022). The parameters input into the software include the datum points, electrode spacing, measurement repetitions, apparent resistivity values, total number of electrodes, and the elevation of each electrode.

The objective of this processing is to visualize the subsurface lithology through a color-contoured image adjusted to the topography of the study area. The input data are inverted to generate a 2D profile that illustrates the distribution of resistivity values beneath the ground surface. The principle of inversion involves matching the field data curves with those generated by the software (Ofterdinger et al., 2019). A lower Root Mean Square (RMS) error indicates a smaller discrepancy between the modeled curve and the actual field data (Chungam et al., 2023). The 2D inverted resistivity sections were analyzed and interpreted based on the specific resistivity ranges for various geological materials established by Telford. To minimize ambiguity, the interpretation was integrated with geological data and preliminary survey findings (Fadilah et al., 2025).

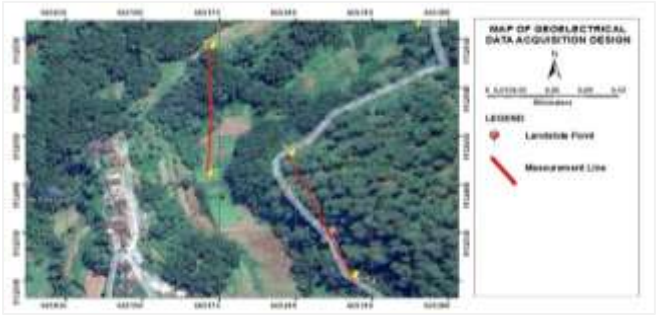

Figure 4. Map of geoelectrical data acquisition design

Result and Discussion

Based on the data processing performed using the HVSR method, the resulting parameters obtained were the dominant frequency (f_0) and the amplification factor (A_0) values. These data were subsequently processed to derive the seismic vulnerability index (Kg) value. The following table presents the f_0, A_0, and Kg values obtained from the measurements:

Table 1. Microseismic Measurement Results

f_0 (Hz)	A_0	Kg (s²/cm)
2.61	4.08	6.38
3.14	3.89	4.81
3.47	9.24	24.57
3.75	4.42	5.211
2.23	2.31	2.39
2.06	6.14	18.27
3.23	3.51	3.82
5.61	3.12	1.73
1.69	5.24	16.24
0.55	1.65	4.91
7.29	5.83	4.67
12.57	4.94	1.94
1.06	4.47	18.84
2.11	3.35	5.31
2.48	4.86	9.53
8.28	1.63	0.32
6.55	3.18	1.55
1.99	3.75	7.05
1.00	3.71	13.72
1.19	4.19	14.74

The seismic vulnerability index is a metric that indicates the level of susceptibility of the surface soil layer to deformation processes. This index serves to predict weak zones on the ground surface, where areas possessing a high seismic vulnerability index consequently bear a high risk of damage (Marfai et al., 2018). Based on the table mentioned above (not shown here), the seismic vulnerability index values range from 0.32 to 24.57. As illustrated in Figure 5 (not shown here), the distribution of these seismic vulnerability index values is categorized into three distinct zones. Zone 1, representing low seismic vulnerability, is denoted by the colors purple to blue, with values ranging from 0.32 to 7.05, encompassing points D1, D2, D4, D5, D7, D8, D10, D11, D12, D14, D16, D17, and D18. Zone 2, representing moderate seismic vulnerability, is marked by the color green, with values ranging from 9.53 to 14.74, covering points D15, D19, and D20. Finally, Zone 3, indicating high seismic vulnerability, is highlighted in orange to red, with values ranging from 16.24 to 24.57, including points D3, D6, D9, and D13.

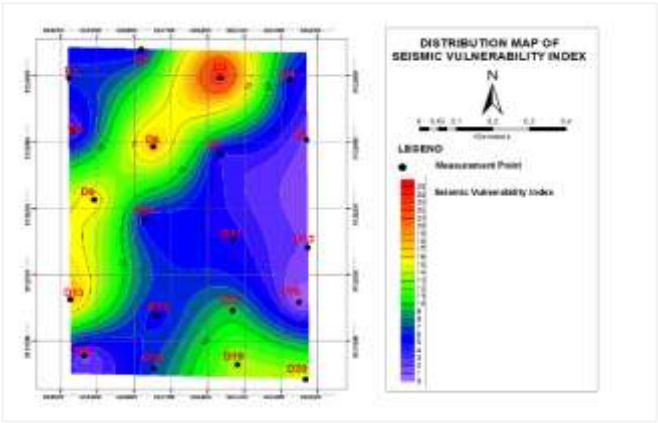

Figure 5. Distribution map of seismic vulnerability index

The highest seismic vulnerability index was observed at point D3, with a value of 24.57 s^2/cm, characterized by a low dominant frequency of 3.47 Hz and a high amplification factor of 9.24. This suggests that the sediment layer in this area consists of thick, soft alluvium that has not yet undergone perfect compaction. A low dominant frequency indicates a significant sediment thickness and a deeper bedrock level (Risa et al., 2023). This material characteristic possesses a high water absorption capacity but low distribution efficiency, making it highly sensitive to vibrations. The resulting volume increase due to water accumulation in this material can trigger landslides (Sasongko et al., 2020). Zones exhibiting both high amplification factors and high seismic vulnerability indices are identified as areas highly susceptible to ground movement (Ferani et al., 2019; Sasongko et al., 2020). A high seismic vulnerability index represents the diminished capacity of a layer to withstand deformation caused by vibrations, thereby increasing the risk of structural damage. Conversely, a low seismic vulnerability index indicates a soil structure capable of attenuating vibrations more effectively (Handayani et al., 2024).

Following the acquisition, processing, and analysis of the microseismic data, a follow-up survey was conducted to measure resistivity values using the geoelectrical method with a dipole-dipole configuration at points exhibiting high seismic vulnerability indices. This stage aimed to characterize the subsurface lithology in the vicinity of those specific locations. Based on the data processing performed with Res2Dinv software, a visual representation of the subsurface resistivity distribution was obtained. Variations in resistivity values represent the subsurface lithological characteristics, which are influenced by porosity, groundwater chemical composition, permeability, as well as the depth and thickness of each geological unit (Rashid et al., 2023).

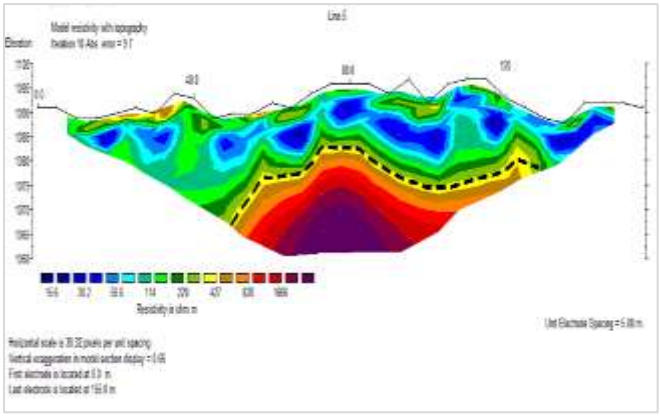

Figure 6. 2D resistivity cross-section of line 5

Table 2. Resistivity Values of 2D Cross-section of Line 5

Resistivity Value (Ωm)	Rock Types
15,6 – 427	Alluvial
428 – 1606	Volcanic Breccia

For Line 5, the interpretation of the 2D cross-section image classifies the resistivity values into two distinct subsurface lithologies. First, the resistivity values ranging from 15.6 to 427 Ωm are interpreted as alluvial. This layer is composed of a mixture of topsoil, tuff, soft soil, mud, humus, silt, gravelly sand, sandy stiff clay, and other materials formed through sedimentation processes with a thickness of ± 10 to 25 meters. Second, the resistivity values from 428 to 1606 Ωm are interpreted as the bedrock (basement rock), which is observed at a depth also ranging approximately from ± 10 to 25 meters.

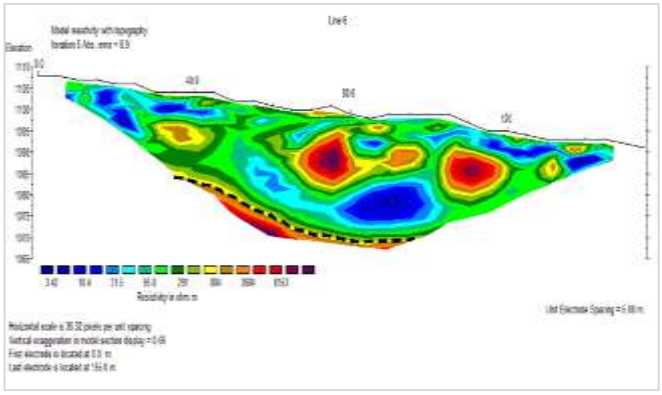

Figure 7. 2D resistivity cross-section of line 6

Table 3. Resistivity Values of 2D Cross-section of Line 6

Resistivity Value (Ωm)	Rock Types
3.42 – 884	Alluvial
885 – 8153	Volcanic Breccia

For Line 6, the interpretation of the 2D cross-section image classifies the resistivity values into two distinct subsurface lithologies. First, resistivity values ranging from 3.42 to 884 Ωm are interpreted as alluvial. This layer is characterized by depositional materials, including topsoil, tuff, soft soil, mud, humus, silt, gravelly sand, sandy stiff clay, and other materials formed through sedimentation processes with a thickness of ± 22.5 meters. Second, resistivity values from 885 to 8153 Ωm are interpreted as the bedrock (basement rock), which is observed at a depth of approximately ± 22.5 meters.

Based on the results from both survey lines, the subsurface lithology in the study area consists of two primary rock units. First, an alluvial layer characterized by low resistivity values with a thickness of up to 25 meters. Second, volcanic breccia identified by high resistivity values, which underlies the alluvial layer and serves as the bedrock. Layers with low resistivity are highly susceptible to landslides, whereas those with high resistivity exhibit greater stability (Sutasoma et al., 2017). These geoelectrical results correlate strongly with the observed microseismic parameters. The significant sediment thickness physically substantiates the low dominant frequency (f_0) of 3.47 Hz. Theoretically, a low frequency indicates a thick sedimentary cover, ranging from 10 to 30 meters, classified as soft soil (Hijriah et al., 2023). The soft and poorly compacted alluvium gives rise to a sharp impedance contrast with the underlying volcanic breccia, thereby triggering a high amplification factor (A_0) of 9.24. The integration of both datasets confirms that point D3 represents the zone with the highest seismic vulnerability index (Kg), resulting from the accumulation of thick, soft sedimentary material over the competent bedrock.

Landslide disasters occurring in the study area are correlated with a combination of local geological conditions and high rainfall intensity. Based on geological data, Brau Hamlet is situated within a geological formation predominantly composed of Quaternary depositional materials. This formation generally consists of alluvium made up of sand-gravel, clay, loam, and other sedimentary components, exhibiting a very low stability level and incomplete consolidation (Kusuma, 2019). Such conditions cause these sedimentary materials to possess high porosity and poor shear stability, consequently creating a high risk of landslides. This occurs because rainwater infiltrating the deposit layers significantly increases the pore water pressure within the material. The resulting increased pore water pressure directly leads to a reduction in effective stress, thereby diminishing the effective shear strength of the soil mass. When the driving force of gravity exceeds the critical threshold of the material's capacity to withstand the driving force within the weak zone (the boundary of the sedimentary layer), the water-laden soil mass loses equilibrium, triggering slope failure and resulting in a landslide disaster.

Conclusion

This study concludes that Gunungsari Village, particularly at point D3, represents the highest landslide risk zone, characterized by a high amplification factor (9.24) and a significant seismic vulnerability index (24.57). Subsurface profiling indicates that this vulnerability is caused by a thick alluvial layer (±10 – 25 meters) consisting of unconsolidated sand, clay, silt, and other sedimentary materials. These materials exhibit low stability and poor consolidation, creating a significant impedance contrast with the underlying bedrock. Generally, the research findings demonstrate that a high Kg value serves as a reliable indicator for identifying zones with thick, soft sedimentary deposits that are prone to slope failure. This implies that infrastructure development must account for the bedrock depth, ranging from 22.5 to 25 meters, to ensure secure foundation piling. Furthermore, the government can utilize these results as a basis for establishing a micro-zonation-based early warning system, prioritizing areas with high seismic vulnerability indices for effective disaster mitigation.

Acknowledgments

The researchers extend their gratitude to all individuals involved in this study for their valuable contribution, cooperation, and support during the execution of this research.

Author Contributions
Conceptualization, I.J.Q. and A.S.; methodology, I.J.Q. and A.S.; validation, A.S. and E.A.S.; formal analysis, I.J.Q.; investigation, I.J.Q.; resources, A.S.; data curation, I.J.Q.; writing-original draft preparation, I.J.Q.; writing-review and editing, A.S. and E.A.S.; visualization, I.J.Q.; supervision, A.S. and E.A.S. All authors have read and agreed to the published version of the manuscript.

Funding
This research received no external funding. The APC was funded by the authors.

Conflicts of Interest
The authors declare no conflict of interest. The research was conducted independently, and the authors had sole responsibility for the design of the study; the collection, analyses, or interpretation of data; the writing of the manuscript; and the decision to publish the results.

References

Alonso-Pandavenes, O., Bernal, D., Torrijo, F. J., & Garzón-Roca, J. (2023). A Comparative Analysis for Defining the Sliding Surface and Internal Structure in an Active Landslide Using the HVSR Passive Geophysical Technique in Pujilí (Cotopaxi), Ecuador. *Land Journal*, *12*(961). https://doi.org/10.3390/land12050961

Batu, B. K. (2025). *Kecamatan Bumiaji dalam Angka* (Vol. 23). BPS Kota Batu.

Chen, S., Lei, J., & Li, Y. (2023). Microtremor Recording Surveys to Study the Effects of Seasonally Frozen Soil on Site Response. *Sensors Journal*, *23*(5573). https://doi.org/10.3390/s23125573

Chen, Y., Yuan, H., Chen, J., Pan, R., Deng, L., Huang, L., Zhang, M., & Yang, Q. (2025). Landslide Early Warning Model Based on Multi-Source Monitoring Data and Unsupervised Machine Learning. *Engineering Applications of Artificial Intelligence*, *164*. https://doi.org/10.1016/j.engappai.2025.113156

Chungam, B., Vinitnantharat, S., & Wangyao, K. (2023). *Evaluation of the Proper Electrode Spacing for ERI Surveys in Open Dumpsites Using Forward Modeling*. *32*(1), 535–545. https://doi.org/10.15244/pjoes/155969

Cintia, J., Br, D., Farduwin, A., & Styawan, Y. (2024). Tanah Di Tanjung Kemala Daerah Kabupaten Tanggamus. *Jurnal Geosaintek*, *10*(2), 106–122. https://doi.org/10.12962/j25023659.v10i2.1619

Demulawa, M., & Daruwati, I. (2021). Analisis Frekuensi Natural Dan Potensi Amplifikasi Menggunakan Metode HVSR (Studi Kasus : Kampus 4 Universitas Negeri Gorontalo). *Edu Research*, *10*(1), 59–63. https://doi.org/10.30606/jer.v10i1.1060

Fadilah, Simarmata, M., Farid, M., & Sukisno. (2025). Estimation of Sustained Groundwater Resource Potential by Analyzing Aquifer Depth Lithology in Selebar Subdistrict , Bengkulu. *Jurnal Penelitian Pendidikan IPA*, *11*(11), 1143–1150. https://doi.org/10.29303/jppipa.v11i11.12799

Febriani, R., Juandi, M., & Islami, N. (2020). Interpretation Geothermal Energy Using Geoelectric Method with Dipole-Dipole in Pawan Village, Rokan Hulu Regency. *Journal of Aceh Physics Society*, *9*(2), 31–36. https://doi.org/10.24815/jacps.v9i2.15304

Ferani, N. A. T., Yuniarto, H. P., & Widyawarman, D. (2019). Analisis Amplifikasi Dan Indeks Kerentanan Seismik Di Kawasan Fmipa Ugm. *Jurnal Geosaintek*, *5*(2). https://doi.org/10.12962/j25023659.v5i2.5726

Gbadebo, A. M., Adeyemi, M. O., Adedeji, H. O., & Badejo, A. A. (2021). Geotechnical and Geomorphological Investigation of Rainfall Induced Shallow Landslide at Okeigbo, Ondo State, Southwestern Nigeria. *Journal of African Earth Sciences*, *178*. https://doi.org/10.1016/j.jafrearsci.2021.104163

Guo, L., Chen, G., Gong, S., Sun, H., & Chantat, K. (2021). Analysis of Rainfall-Induced Landslide Using the Extended DDA by Incorporating Matric Suction. *Computers and Geotechnics*, *135*. https://doi.org/10.1016/j.compgeo.2021.104145

Haerudin, N., Alami, F., & Rustadi. (2019). *Mikroseismik, Mikrotremor dan Microearthquake dalam Ilmu Kebumian*. Pusaka Media.

Handayani, W., & Sekarsari, N. H. (2024). Analisis Kerentanan Tanah di Selatan Zona Longsor Desa Kalongan, Kabupaten Semarang Menggunakan Metode HVSR. *Jurnal Stasiun Geofisika Sleman*, *2*(2), 1–6. Retrieved from https://jurnal.stageofsleman.id/index.php/jsgs/article/view/22

Hijriah, Sila, A. A., Isdyanto, A., Ola, M. N. La, Hamdi, F., Masgode, M. B., Aryadi, A., Dzakir, L. O., Astari, M. D., & Buarlele, L. (2023). *Dinamika dan Struktur Tahan Gempa*. Tohar Media.

Himi, M., Anton, M., Sendr, A., Ercoli, M., Deidda, G. P., Urruela, A., & Casas, A. (2022). Application of Resistivity and Seismic Refraction Tomography for Landslide Stability Assessment in Vallcebre, Spanish Pyrenees. *Remote Sensing Journal*, *14*(6333). https://doi.org/10.3390/rs14246333

Januarta, G. H., Yudistira, T., Tohari, A., & Fattah, E. I. (2020). Mikrozonasi Seismik Wilayah Padalarang, Kabupaten Bandung Barat Menggunakan Metode Horizontal To Vertical Spectral Ratio (HVSR). *RISET Geologi Dan Pertambangan*, *30*(2), 143. https://doi.org/10.14203/risetgeotam2020.v30.1087

Karimah, K., Susilo, A., Suryo, E. A., Rofiq, A., & Hasan, M. F. R. (2022). Analysis of Potential Landslide Areas Using Geoelectric Methods of Resistivity in The Kastoba Lake, Bawean Island, Indonesia. *Jurnal Penelitian Pendidikan IPA*, *8*(2), 660–665. https://doi.org/10.29303/jppipa.v8i2.1414

Krylov, A. A., Kulikov, M. E., Kovachev, S. A., Medvedev, I. P., Lobkovsky, L. I., & Semiletov, I. P. (2022). Peculiarities of the HVSR Method Application to Seismic Records Obtained by Ocean-Bottom Seismographs in the Arctic. *Applied Sciences Journal*, *12*(9576). https://doi.org/10.3390/app12199576

Liao, M., Wen, H., & Yang, L. (2022). Identifying the essential conditioning factors of landslide susceptibility models under different grid resolutions using hybrid machine learning: A case of Wushan and Wuxi counties, China. *Catena*, *217*. https://doi.org/10.1016/j.catena.2022.106428

Marfai, M. A., Mardiatno, D., & Sunarto. (2018). *Penaksiran Multirisiko Bencana di Wilayah Kepesisiran Parangtritis: alam Era Teknologi Informasi dan Komunikasi*. UGM Press.

Masitoh, F., Rusydi, A. N., & Pratama, I. D. (2019). Kajian hidrogeomorfologi pada DAS orde 0 (nol) di Dusun Brau Kota Batu. *Jurnal Pendidikan Geografi: Kajian, Teori, Dan Praktik Dalam Bidang Pendidikan Dan Ilmu Geografi*, *24*(2). https://doi.org/10.17977/um017v24i22019p073

Moradi, S., Heinze, T., Budler, J., Gunatilake, T., Kemna, A., & Huisman, J. A. (2021). Combining Site Characterization, Monitoring and Hydromechanical Modeling for Assessing Slope Stability. *Land Journal*, *10*(423), 1–23. https://doi.org/10.3390/land10040423

Novianti, D. (2019). *Implementasi Teori "Cracked Soil" Pada Identifikasi Kelongsoran*. Jakad Media Publishing.

Ofterdinger, U., MacDonald, A. M., Comte, J. C., & Young, M. E. (2019). *Groundwater in Fractured Bedrock Environments: Managing Catchment and Subsurface Resources*. Geological Society of London.

Pourghasemi, H. R., Gayen, A., Edalat, M., Zarafshar, M., & Tiefenbacher, J. P. (2020). Is Multi-Hazard Mapping Effective in Assessing Natural Hazards and Integrated Watershed Management. *Geoscience Frontiers*, *11*(4), 1203–1217. https://doi.org/10.1016/j.gsf.2019.10.008

Rananda, E., Prabowo, L., Prabowo, A. P., Rasimeng, S., & Yogi, I. B. S. (2020). Analysis and Zonation of Land Vulnerability Areas in Pekon Karangrejo Ulubelu Tanggamus Using Microzonation Method. *Jurnal Geofisika*, *18*(1), 14. https://doi.org/10.36435/jgf.v18i1.420

Rashid, M., Kamran, M., Zeb, M. J., Islam, I., Janjuhah, H. T., & Kontakiotis, G. (2023). Assessment of Potential Potable Water Reserves in Islamabad , Pakistan Using Vertical Electrical Sounding Technique. *Hydrology Journal*, *10*(217). https://doi.org/10.3390/hydrology10120217

Rif'ah, K. D., Jamil, A. M. M., Suwito, S., & Kurniawati, D. (2024). Pemetaan Tingkat Kerawanan Bencana Tanah Longsor Menggunakan Metode Weighted Overlay di Kecamatan Poncokusumo Kabupaten Malang. *Journal of Geographical Sciences and Education*, *02*(4). https://doi.org/10.69606/geography.v2i4.137

Risa, I. N., Maison, & Dewi, I. K. (2023). Analisis Kerentanan Tanah Berdasarkan Pengukuran Mikrotremor Di Desa Jati Mulyo, Tanjung Jabung Timur. *Jurnal Geofisika Eksplorasi*, *09*(01). https://doi.org/10.23960/jge.v9i1.236

Rizzo, E., Giampaolo, V., Capozzoli, L., De Martino, G., Romano, G., Santilano, A., & Manzella, A. (2022). 3D deep geoelectrical exploration in the Larderello geothermal sites (Italy). *Physics of the Earth and Planetary Interiors*, *329–330*. https://doi.org/10.1016/j.pepi.2022.106906

Santosa, S., & Suwarti, T. (1992). *Peta Geologi Lembar Malang, Jawa*. Pusat Penelitian dan Pengembangan Geologi.

Sasongko, D. P., Yuliyanto, G., & Zaenal, A. (2020). Karakterisasi Daerah Rawan Gerakan Tanah Di Lapangan Pandanmurti Desa Candigaron Kecamatan Sumowono Kabupaten Semarang Dengan Metode Mikrotremor. *Jurnal Pembangunan Wilayah Dan Kota*, *16*(2), 136–143. https://doi.org/10.14710/pwk.v16i2.26401

Stark, T. D., Estes, K. D., Silver, R. C., Holman, E. A., Leshchinsky, B. A., & Vahedifard, F. (2025). Objective versus Subjective Landslide Risk: A Case of Cache Creek Landslide in California. *International Journal of Disaster Risk Reduction*. https://doi.org/10.1016/j.ijdrr.2025.105910

Susilo, A., & Wiyono, S. H. (2012). Frequency Analysis and Seismic Vulnerability Index by Using Nakamura Methods at a New Artery Way in Porong,Sidoarjo, Indonesia. *International Journal of Applied Physics and Mathematics*, *2*(4), 227–230. https://doi.org/10.7763/IJAPM.2012.V2.97

Susilo, A., Zulaikah, S., Fauzi, A., Ilham, Ma'muri, Wirawan, K., Haniyyah, S., Zarkoni, A., Persada, Y. D., Bery, A. A., & Hasan, M. F. R. (2026). Seismic site characterization of Malang Regency (Indonesia) using HVSR inversion. *Kuwait Journal of Science*, *53*(1), 100486. https://doi.org/10.1016/j.kjs.2025.100486

Sutasoma, M., Susilo, A., & Suryo, E. A. (2017). Penyelidikan Zona Longsor dengan Metode

Resistivitas dan Analisis Stabilitas Lereng untuk Mitigasi Bencana Tanah Longsor. *Indonesian Journal of Applied Physics*, *7*(1), 35. https://doi.org/10.13057/ijap.v7i1.8784

Syamsuddin, E., & Assegaf, M. A. H. (2021). *Dasar-Dasar Akuisisi Data MASW dan Mikrotremor*. Unhas Press.

Yue, M., & Zhou, G. (2024). Assessment Rainfall-Induced Landslides Using Arbitrary Dipole – Dipole Direct Resistivity Configuration. *Applied Sciences Journal*, *14*(9096). https://doi.org/10.3390/app14199096

Yuliawati, W. S., Rasimeng, S., & Karyanto. (2019). Pengolahan Data Mikrotremor Berdasarkan Metode Hvsr Dengan Menggunakan Matlab. *Jurnal Geofisika Ekplorasi*, *5*(1), 45–59. https://doi.org/10.23960/jge.v5il.22

Zevallos, A., Torres, J., Segura, C., & Carrasco, J. (2025). Geoelectrical Characterization of Sedimentary Landslides in the Laguna Del Amor Area, Chota-Cajamarca (Peru). *Applied Sciences Journal*, *15*(2327). https://doi.org/10.3390/app15052327

Zhang, B., Zhang, M., Liu, H., Sun, P., Feng, L., Li, T., & Wang, Y. (2022). Water Flow Characteristics Controlled by Slope Morphology under Different Rainfall Capacities and Its Implications for Slope Failure Patterns. *Water Journal*, *14*(1271). https://doi.org/10.3390/w14081271